More on the Surface State of Expanding Champagne Bubbles Rising at Intermediate Reynolds and High Peclet Numbers

ARTICLE *in* LANGMUIR · JANUARY 2003

Impact Factor: 4.46 · DOI: 10.1021/la026594w

2 AUTHORS:

Gérard Liger-Belair
French National Centre for Scientific Research
85 PUBLICATIONS **964** CITATIONS

SEE PROFILE

Philippe Jeandet
Université de Reims Champagne-Ardenne
150 PUBLICATIONS **3,825** CITATIONS

SEE PROFILE

More on the Surface State of Expanding Champagne Bubbles Rising at Intermediate Reynolds and High Peclet Numbers

Gérard Liger-Belair* and Philippe Jeandet

Laboratoire d'Œnologie, UPRES EA 2069, Faculté des Sciences de Reims, B.P. 1039, 51687 Reims Cedex 2, France

Received September 23, 2002. In Final Form: November 20, 2002

Bubbles rising in a glass poured with carbonated beverage constitute a daily example of rising and expanding bubbles. By measuring both the drag coefficients and the Sherwood numbers of ascending champagne bubbles during their rise toward the free surface, we provided evidence that, contrary to bubbles of fixed or shrinking radii, expanding champagne bubbles experience a transient regime during ascent, where the bubble behavior progressively changes from that of a rigid sphere to that of a fluid sphere. The progressive gain of interfacial mobility during bubble ascent was interpreted as a dilution of the surface-active compounds on the rising bubble due to the continuous bubble growth. Time scales of bubble expansion and surfactant adsorption were estimated during the rise and found to be in quite good accordance with our experimental results at low Reynolds numbers.

1. Introduction

Since rising bubbles are of fundamental importance in many natural and industrial processes, rising bubble dynamics has been thoroughly investigated by a wide range of scientists (chemical and mechanical engineers, geophysicists, oceanographers, etc.).

As first noticed by Bond,[1] the hydrodynamics of rising bubbles strongly depends on the presence of surface-active substances in the liquid medium. During ascent, surface-active materials progressively accumulate at the rear part of the rising bubble, thus increasing the immobile area of the bubble surface. A surface concentration gradient ensues between the front and the rear part of the bubble, which induces a modification of the hydrodynamic boundary conditions on the bubble via the onset of the so-called Marangoni effect. The gradient of surface tension around the rising bubble induces a viscous shear stress which reduces its interfacial mobility. Viscous dissipation is therefore enhanced, which leads to a lower rising velocity. This model based on the rigidification of the rear part of the bubble is known as the stagnant cap model. Numerous experimental, numerical, and theoretical studies on bubble motion have already confirmed this phenomenon.[2−14] Hydrodynamically speaking, a rising bubble rigidified by surfactants runs into more resistance than a bubble presenting a more flexible interface free from surface-active materials. Therefore, the drag coefficient experienced by a bubble of a fixed radius rising in a surfactant solution progressively enhances since the surface of the stagnant cap progressively increases. Bubbles of fixed radii ascending in surfactant solutions therefore experience a transient regime, where the bubble behavior progressively changes from that of a fluid to that of a rigid sphere. Recently, Takemura and Yabé[13,14] thoroughly examined the velocity and dissolution rate of shrinking carbon dioxide bubbles rising in slightly contaminated water. They also found that shrinking bubbles experienced a transient regime in terms of interfacial mobility, where the bubble behavior changes from that of a fluid to that of a rigid sphere.

The case of a rising and expanding bubble is a little bit more subtle than that of a bubble of a fixed radius or a shrinking bubble. Since the bubble expands during its rise through the supersaturated liquid, the bubble interface continuously increases and therefore continuously offers newly created surface to the adsorbed surface-active materials. Expanding bubbles therefore experience a competition between two opposing effects. As a result, if the rate of dilatation of the growing bubble overcomes the rate at which surface-active molecules stiffen the bubble surface, a rising bubble progressively "cleans" its interface. On the contrary, if the rising bubble interface increases at a lower rate than the rate at which surfactants adsorb on its surface, the surface concentration of surfactants progressively increases, resulting in a progressive rigidification of the bubble surface.

To investigate the rise velocity of expanding gas bubbles in surfactant solutions, we decided to first focus on the fantastic and daily example of rising and expanding bubbles illustrated by streams of bubbles in champagne wines. Actually, champagne wines contain a non-negligible amount of surface-active compounds such as proteins and glycoproteins in the range of several milligrams per liter.[15−17] Since champagne is supersaturated with carbon dioxide dissolved molecules, bubbles nucleated on the glass wall impurities continue to expand during ascent, at

* Corresponding author. Tel/fax: 00 (33)3 26 91 33 40. E-mail: gerard.liger-belair@univ-reims.fr.

(1) Bond, V. N. *Philos. Mag.* **1927**, *4*, 889.
(2) Levich, V. G. *Physicochemical Hydrodynamics*; Prentice Hall: Englewood Cliffs, NJ, 1962.
(3) Davis, R. E.; Acrivos, A. *Chem. Eng. Sci.* **1966**, *21*, 681−685.
(4) Aybers, N. M.; Tapuccu, A. *Waerme Stoffuebertrag.* **1969**, *2*, 118−128.
(5) Harper, J. F. *J. Fluid Mech.* **1973**, *58*, 539−545.
(6) Duineveld, P. C. Bouncing and coalescence of two bubbles in water. Ph.D. Thesis, University of Twente, Enschede, The Netherlands, 1994.
(7) McLaughlin, J. B. *J. Colloid Interface Sci.* **1996**, *184*, 614−625.
(8) Cuenot, B.; Magnaudet, J.; Spennato, B. *J. Fluid Mech.* **1997**, *339*, 25−53.
(9) Ybert, C.; di Meglio, J.-M. *Eur. Phys. J. B* **1998**, *4*, 313−319.
(10) Ybert, C. Stabilisation des mousses aqueuses par des protéines. Ph.D. Thesis, Université Louis Pasteur, Strasbourg, France, 1998.
(11) Ybert, C.; di Meglio, J.-M. *Eur. Phys. J. E* **2000**, *3*, 143−148.
(12) Zholkovskij, E. K.; Koval'chuk, V. I.; Dukhin, S. S.; Miller, R. *J. Colloid Interface Sci.* **2000**, *226*, 51−59.
(13) Takemura, F.; Yabé, A. *Chem. Eng. Sci.* **1998**, *53*, 2691−2699.
(14) Takemura, F.; Yabé, A. *J. Fluid Mech.* **1999**, *378*, 319−334.

10.1021/la026594w CCC: $25.00
Published on Web 01/11/2003

growth rates of several hundred micrometers per second, by continuous diffusion of CO_2 into the rising bubbles. Expanding champagne bubbles therefore accelerate when rising toward the liquid surface.[18,19] The decrease of hydrostatic pressure between the nucleation site in the bottom of the glass and the free surface (around 10 cm) is completely negligible. It causes the bubble volume to grow only about 1%. Recently, by measuring the drag coefficients experienced by expanding champagne bubbles during their way up and by comparing them with empirical drag coefficients found in the huge literature devoted to bubbles of various sizes ascending through various liquids, we provided evidence that champagne bubbles showed a behavior intermediate between that of a rigid and that of a fluid sphere.[18]

In this paper, both the drag coefficient and the Sherwood number of ascending champagne bubbles were investigated with increasing bubble Reynolds numbers all along the rise. Our experimental data were compared with previous empirical relationships derived for the two extreme boundary regimes likely to be experienced by a rising bubble, that is, a fully mobile interface free from surface-active compounds on one hand and a rigid, contaminated interface on the other hand. Contrary to the case of rising bubbles of fixed radii or shrinking bubbles, this new set of experimental data strongly suggests that expanding and rising champagne bubbles experience a transient regime during ascent, where the bubble behavior progressively changes from that of a rigid sphere to that of a fluid sphere.

2. Experimental Section

2.1. Materials. For these experiments, we chose a standard commercial champagne wine supplied by our industrial partner. We also used a classical cylindrical crystal flute with a diameter of 4.9 cm and a wall thickness of 0.8 mm. Prior to each experiment, the flute was rinsed several times using distilled water and then air-dried. Physicochemical parameters of champagne were determined at 20 °C with a sample of champagne first degassed. The champagne density ρ was measured and found to be equal to 998 kg m^{-3}. The champagne kinematic viscosity η was measured with an Ubbelhode capillary viscosimeter (type 501 10/I) and found to be equal to 1.66×10^{-3} kg m^{-1} s^{-1}. Champagne is obviously not a pure liquid. It is a complex hydroalcoholic solution containing, in addition to ethanol, tens of aromatic compounds and a non-negligible amount of surface-active macromolecules (mostly composed of proteins and glycoproteins) in the range of several milligrams per liter.[15−17] The protein content was quantified by spectrocolorimetry, using a modified Bradford procedure with bovine serum albumin (BSA) as the standard protein.[20,21] We found a concentration, C, of protein in the champagne bulk of approximately 5 mg L^{-1}.

Bubble production in a glass poured with champagne was already shown[22,23] to be a type IV nucleation process (according to the classification of Jones et al.[24]), meaning that in order to nucleate and grow freely, a bubble needs a pre-existing gas cavity (the so-called nucleation site) with a radius of curvature greater than the critical radius of homogeneous nucleation. It was recently found that most of the nucleation sites are located on tiny and hollow cellulose-fiber-made structures of the order of 100 μm with a cavity mouth of several micrometers.[23] By entrapping a gas pocket when champagne is poured into the glass, such particles are responsible for the repetitive and clockwork production of bubbles that rise in-line in the form of elegant bubble trains.

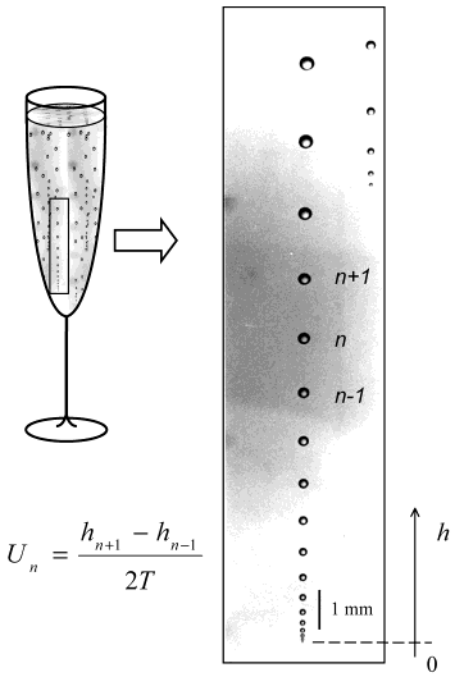

Figure 1. Determination of the rising velocity of bubbles during ascent from the enlarged photograph of a single bubble train and from the period of bubble production, T, as determined with strobe lighting (ref 18). The velocity U_n of the nth bubble of the bubble train may be deduced from the position of the one that just precedes, indexed $n + 1$, and the one that just follows, indexed $n - 1$.

2.2. Experimental Setup. We were tempted to use the clockwork repetitive bubble production from nucleation sites to develop a simple experimental setup able to follow the motion of bubbles in the flute poured with champagne. This experimental setup was already thoroughly described in a previous research article.[18] To resume in a few words, we benefited from the clockwork repetitive bubble production from nucleation sites to develop a simple but reliable method, which consists of the association of a photo camera with a stroboscopic light. Actually, since bubbles are released from nucleation sites with clockwork regularity, the photograph of each bubble train can be treated as a succession of pictures of the same bubble separated from the period of bubble formation, T, as determined by equaling the bubble formation frequency of a given bubble train with the frequency of strobe lighting. The photograph displayed in Figure 1 illustrates how to measure the increasing bubble velocity along its rise toward the free surface. The longest bubble trains were of the order of 10 cm. To eliminate the influence of the initial liquid convection when champagne is poured into the glass, observation of the bubble trains (strobe lighting and photography) was conducted at least 3 min after pouring. Experiments were performed at room temperature (20 ± 2 °C).

In the following, changes with time along the bubble rise will be measured by approaching the differential quantity, dt, by the short time interval, T, between two successive bubbles. For example, the bubble growth rate during ascent, $dR/dt = \dot{R}$, is approached by measuring the quantity $\Delta R/T$ for each couple of

(15) Dussaud, A. Etude des propriétés de surface statiques et dynamiques de solutions alcooliques de protéines: Application à la stabilité des mousses de boissons alcoolisées. Ph.D. Thesis, ENSIAA, Massy, France, 1993.
(16) Brissonnet, F.; Maujean, A. *Am. J. Enol. Vitic.* **1993**, *44*, 297−301.
(17) Marchal, R.; Bouquelet, S.; Maujean, A. *J. Agric. Food Chem.* **1996**, *44*, 1716−1722.
(18) Liger-Belair, G.; Marchal, R.; Robillard, B.; Dambrouck, T.; Maujean, A.; Vignes-Adler, M.; Jeandet, P. *Langmuir* **2000**, *16*, 1889−1895.
(19) Liger-Belair, G. *Ann. Phys.* (*Paris*) **2002**, *27* (4), 1−106.
(20) Bradford, M. M. *Anal. Biochem.* **1976**, *72*, 248−254.
(21) Marchal, R.; Seguin, V.; Maujean, A. *Am. J. Enol. Vitic.* **1997**, *48*, 333−337.
(22) Liger-Belair, G.; Vignes-Adler, M.; Voisin, C.; Robillard, B.; Jeandet, P. *Langmuir* **2002**, *18*, 1294−1301.
(23) Liger-Belair, G.; Marchal, R.; Jeandet, P. *Am. J. Enol. Vitic.* **2002**, *53*, 151−153.
(24) Jones, S. F.; Evans, G. M.; Galvin, K. P. *Adv. Colloid Interface Sci.* **1999**, *80*, 27−50.

Table 1. Relationships, Derived for Both Rigid and Fluid Sphere Conditions, between the Drag Coefficient and the Reynolds Number of Ascending Bubbles[a]

authors	range of validity	relationship for C_D(Re)	bubble surface state
Schiller and Naumann (see Clift et al., ref 25)	(Re < 800)	$C_{RS} = \frac{24}{Re}(1 + 0.15Re^{0.687})$	rigid
Magnaudet et al. (ref 26)	(Re < 50)	$C_{FS} = \frac{16}{Re}(1 + 0.15\sqrt{Re})$	fluid
Maxworthy et al. (ref 27)	(1 < Re < 800)	$C_{FS} = 11.1Re^{-0.74}$	fluid

[a] The subscripts RS and FS refer to the rigid and fluid sphere boundary conditions, respectively.

successive bubbles in a bubble train, ΔR being the radius increase between two successive bubbles.

3. Results and Discussion

3.1. Drag Coefficients of Ascending Champagne Bubbles. Generally speaking, bubbles rising in liquid media induce a displacement of the surrounding fluid, which leads to an added-mass force. Finally, the velocity of a rising bubble follows from a force balance between inertia of liquid displaced, buoyancy, and drag force,

$$\frac{d}{dt}(mU) = \frac{4}{3}\pi R^3 \rho g - \frac{1}{2}C_D \rho U^2 \pi R^2 \qquad (1)$$

where m is the added mass of the bubble equal to the mass of liquid displaced around the rising bubble, R and U are respectively the radius and the velocity of ascending bubbles, g is the acceleration due to gravity, ρ is the liquid density, and C_D is the drag coefficient.

However, it has already been shown in a previous research article that the added-mass force experienced by a champagne bubble during its way up remains very low in comparison with its buoyancy.[18] As a result, inertia can be neglected and the equation of motion reduces itself to a simple balance between buoyancy and drag force, which allows a simple experimental determination of the drag coefficient experienced by champagne bubbles through the expression

$$C_D = \frac{8gR}{3U^2} \qquad (2)$$

The close examination of numerous bubble trains enabled us to cover a range of bubble radii between approximately 40 μm (after the bubble detachment from nucleation sites) and 480 μm (near the free surface), resulting in intermediate Reynolds numbers ($Re = 2\rho RU/\eta$) increasing from approximately 10^{-1} to 10^2 and high Peclet numbers ($Pe = 2RU/D$) increasing from approximately 10^2 to 10^5, D being the diffusion coefficient of dissolved CO_2 molecules in the champagne bulk. High Peclet numbers suggest, all along the bubble rise, that mass transfer phenomena are governed by convection and not by pure diffusion. For numerous bubble trains, the drag coefficient of ascending bubbles was determined from eq 2 all along the bubble rise with increasing Re.

The hydrodynamics of bubbles rising at low Re is quite well understood, but the case of bubbles rising at intermediate and high Re is much more complicated due to difficulties such as flow separation from Re ≈ 20. The hydrodynamics of bubbles rising in this range of Re cannot be studied analytically and is therefore accessible only through numerical simulation and experimental approaches. During the past decades, many empirical or semiempirical relations have been proposed to correlate C_D with Re for bubbles in free rise. Some of the most popular are listed in the book by Clift et al.[25] Our experimental measurements of C_D(Re) are to be compared with the drag coefficients experienced by a bubble in the two limiting boundary regimes in terms of interfacial mobility (on one hand, a rising bubble free from surface-active substances presenting a full interfacial mobility, and on the other hand, a contaminated bubble that has a zero velocity boundary condition for the external fluid and that hydrodynamically behaves as a rigid sphere of the same density and the same diameter). We therefore retrieved three empirical drag coefficients C_D(Re) that are listed in Table 1. We chose these relationships among many others, since they are proposed with an accuracy better than 6% compared with their authors' experimental data and since they are available in the range of Re covered by champagne bubbles. To indirectly access the champagne bubble surface state during ascent, the normalized drag coefficient C_D*(Re) defined as follows was used:

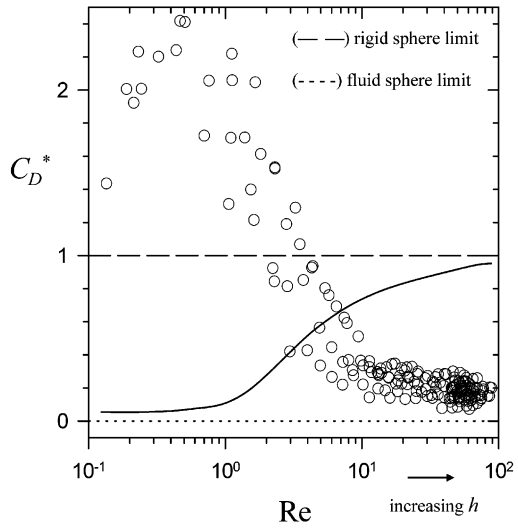

Figure 2. Normalized drag coefficient C_D*(Re) experienced by expanding champagne bubbles during ascent (○), compared with the normalized drag coefficient that a bubble of fixed radius or a shrinking bubble rising in a surfactant solution would experience (solid line); the fluid (short-dashed line) and rigid (long-dashed line) sphere limits are also presented.

$$C_D^* = \frac{(C_D - C_{FS})}{(C_{RS} - C_{FS})} \qquad (3)$$

where C_{RS} and C_{FS} are well-known empirical drag coefficients derived for rigid and fluid sphere conditions, respectively (see Table 1). Therefore, bubbles with a fully mobile interface behaving hydrodynamically as fluid spheres will exhibit values of C_D* close to zero, whereas polluted bubbles behaving hydrodynamically as rigid spheres will have values of C_D* close to 1.

In Figure 2, C_D*(Re) was plotted all along the bubble rise, for bubbles of various bubble trains. At low Re (Re

(25) Clift, R.; Grace, J. R.; Weber, M. E. *Bubbles, Drops and Particles*; Academic Press: New York, 1978.

$\lesssim 1$), just after the bubble detachment from a nucleation site stuck on the glass wall, C_D* is significantly higher than the rigid sphere limit. Actually, during the very first moments after detachment from the nucleation site, wall effects are certainly not negligible and probably modify the liquid flow around the rising bubble, resulting in a significant increase of the drag coefficient experienced by the bubble. Then, from Re $\approx$ 1 to Re $\approx$ 10, C_D* quickly decreases from the rigid sphere limit to an intermediate value close to the fluid sphere limit, thus suggesting that the champagne bubble interface progressively increases its mobility. From Re $\approx$ 10 to Re $\approx$ 100, C_D* remains quite low, which suggests that champagne bubbles have reached a quasi-stationary stage in terms of interfacial mobility. Strictly speaking, the level of the plateau seems to slightly decrease during this second quasi-stationary stage, which means that the bubble interface could continue to very progressively increase its mobility. In Figure 2, the line which progressively rises from the fluid to the rigid sphere limit qualitatively symbolizes the transient regime that a bubble of a fixed radius rising in a surfactant solution would experience. Such a transient regime, where the bubble interface progressively changes from that of a fluid to that of a rigid sphere, was also experimentally and numerically evidenced for shrinking bubbles rising in slightly contaminated water.[13,14] In the case of shrinking bubbles rising in surfactant solutions, the progressive decrease of the rising bubble area concentrates surface-active materials at the bubble surface and even accelerates the contamination process of the bubble interface.

In the present situation, the main features of experimental C_D*(Re) in Figure 2 strongly suggest that, contrary to a bubble with a fixed or a shrinking radius, the expanding champagne bubble interface experiences a transient regime during its way up, where the bubble interface progressively changes its mobility from that of a rigid to that of a fluid sphere. We are logically tempted to attribute this gain of interfacial mobility during ascent to the bubble growth which continuously offers newly created surface to the adsorbed surface-active materials, thus diluting surface-active compounds on ascending bubbles.

In a way, by continuously growing during ascent, champagne bubbles would "clean up" themselves. Another experimental method which should confirm or refute this hypothesis would be welcomed. Let us examine more closely the bubble growth during the bubble rise.

3.2. Mass Transfer of CO_2 Molecules during Ascent. The carbon dioxide molecule flux, $\vec{J}$, through the interface of a rising champagne bubble, which is responsible for its continuous growth, is a combination of the diffusive and convective fluxes and is locally expressed by the first and second Fick's laws as

$$\begin{cases} \vec{J} = c\vec{V} - D\vec{\nabla c} \\ \dfrac{\partial c}{\partial t} = \mathrm{div}(D\cdot\vec{\nabla c}) - \mathrm{div}(c\vec{V}) \end{cases} \quad (4)$$

where $\vec{V}$ and $\vec{\nabla c}$ are respectively the velocity of the liquid flow and the concentration gradients of CO_2 molecules in the boundary layer around the rising bubble, D being in the present situation the diffusion coefficient of CO_2 molecules in the champagne bulk.

Since the velocity gradient distribution in the close vicinity of a rising bubble is strongly affected by the presence of surface-active compounds adsorbed at the bubble surface, mass transfer, which also strongly depends on fluid convection via the convective fluxes $c\vec{V}$, also significantly depends on the bubble surface state (for an exhaustive review, see the book by Clift et al.[25]). It would certainly be very instructive to compare the experimental mass transfer of CO_2 molecules experienced by a champagne bubble with that related to the two limiting hydrodynamic situations, that is, a rising bubble with a fully mobile interface on one hand and a rising bubble with a rigid interface on the other hand.

Generally speaking, in the literature devoted to mass transfer phenomena associated with bubbles and drop dynamics, heat and mass transfer are presented by use of the two dimensionless Sherwood and Peclet numbers,

$$\mathrm{Sh} = \frac{2RK}{D} \quad \text{and} \quad \mathrm{Pe} = \frac{2RU}{D} = \mathrm{ScRe} \quad (5)$$

where K is the mass transfer coefficient and Sc is the Schmidt number (Sc $= \eta/D\rho$). The mass transfer coefficient K is defined from the general equation that governs the mass flux through an interface,

$$\frac{\mathrm{d}N}{\mathrm{d}t} = -KA\Delta c \quad (6)$$

where N is the number of transferred molecules, A is the interface area, and Δc (the driving force of mass transfer) is the difference in molecular concentration of dissolved carbon dioxide between the liquid bulk far from the interface, denoted c_∞, and that in the boundary layer close to the interface in equilibrium with the gaseous carbon dioxide of the rising bubble, denoted c_0. Since we are dealing with spherical bubbles, the latter relation can be transformed as follows by use of the equation of state of the gas supposed to behave ideally in the rising bubble,

$$\frac{\mathrm{d}N}{\mathrm{d}t} = \frac{P_B\dot{V} + \dot{P}_B V}{k_B\theta} = -4\pi R^2 K(c_\infty - c_0) \quad (7)$$

where P_B is the pressure inside the bubble, V is the bubble volume, k_B is the Boltzmann constant, and θ is the absolute temperature. Due to both hydrostatic and capillary pressures, the pressure inside a rising bubble slightly exceeds the atmospheric pressure P_0 ($P_B = P_0 + \rho gz + 2\gamma/R$), z being the depth of liquid above the rising bubble. Therefore, $\dot{P}_B = -\rho gU - 2\gamma\dot{R}/R^2$. The ratio of $\dot{P}_B V$ to $P_B\dot{V}$ was nevertheless estimated from our experimental data all along the bubble rise. It never exceeded $\dot{P}_B V/P_B\dot{V} \approx 10^{-2}$. As a result, with our experimental conditions (bubble sizes and bubble growth rates), the term $\dot{P}_B V$ in eq 7 will be neglected afterward. Finally, by replacing K in eq 7 by its expression as a function of the Sherwood number and by simplifying, we can rewrite Sh as follows:

$$\mathrm{Sh} \approx \frac{2P_0}{D(c_\infty - c_0)k_B\theta} R\dot{R} \propto R\dot{R} \quad (8)$$

Due to bubbling and diffusion through the flat free surface of the liquid, carbon dioxide molecules progressively escape from the liquid medium. Consequently, c_∞ progressively decreases and cannot be considered as a constant as time proceeds. Since the observation of bubble trains was conducted at different steps of gas discharging and since c_∞ is not measured in the present report, the exact value of the experimental Sh is not completely accessible. Nevertheless, the carbon dioxide content in the bulk, c_∞, may be considered as a constant for the treatment of experimental data associated with each given nucleation site, since the time of ascent of a champagne bubble is very short ($\approx$1 s). Therefore, for a given bubble train, the experimental determination of the bubble radius

Table 2. Relationships, Derived for Both Rigid and Fluid Sphere Conditions, between the Sherwood Number and the Reynolds Number of Ascending Bubbles[a]

authors	range of validity	relationship for Sh(Re)	bubble surface state
Clift et al. (ref 25)	(Re < 1)	$Sh_{RS} = 1 + (1 + ScRe)^{1/3}$	rigid
Clift et al. (ref 25)	(1 < Re < 100)	$Sh_{RS} = 1 + (1 + ScRe)^{1/3}Re^{0.077}$	rigid
Clift et al. (ref 25)	(Re < 1)	$Sh_{RS} = 1 + (1 + 0.564(ScRe)^{2/3})^{3/4}$	fluid
Abdel-Alim and Hamielec (ref 28)	(1 < Re < 100)	$Sh_{FS} = \frac{2}{\sqrt{\pi}}\left(1 - \frac{0.67}{\left(1 + \left(\frac{2Re^{0.5}}{8.67}\right)^{4/3}\right)^{3/4}}\right)^{1/2}(ScRe)^{1/2}$	fluid

[a] The subscripts RS and FS refer to the rigid and fluid sphere boundary conditions, respectively.

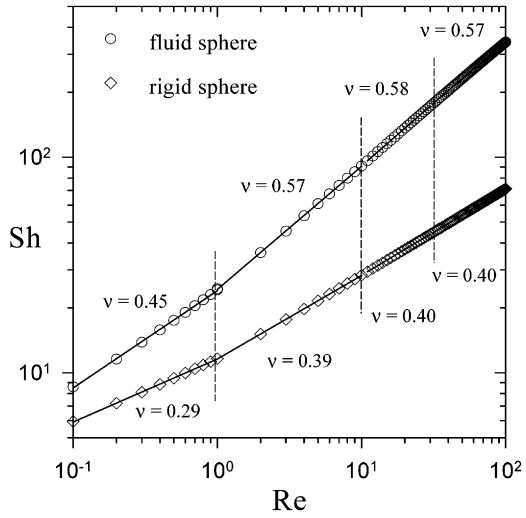

Figure 3. Theoretical (for Re < 1) and empirical relationships (for Re > 1) previously derived for Sh(Re), respectively for rigid and fluid sphere conditions. The whole range of Re experienced by expanding champagne bubbles was divided into four parts, and the corresponding relationships Sh(Re) in the corresponding ranges of Re were independently fitted by power laws; the critical exponents of the respective power laws appear close to the corresponding curves, for both rigid and fluid sphere conditions.

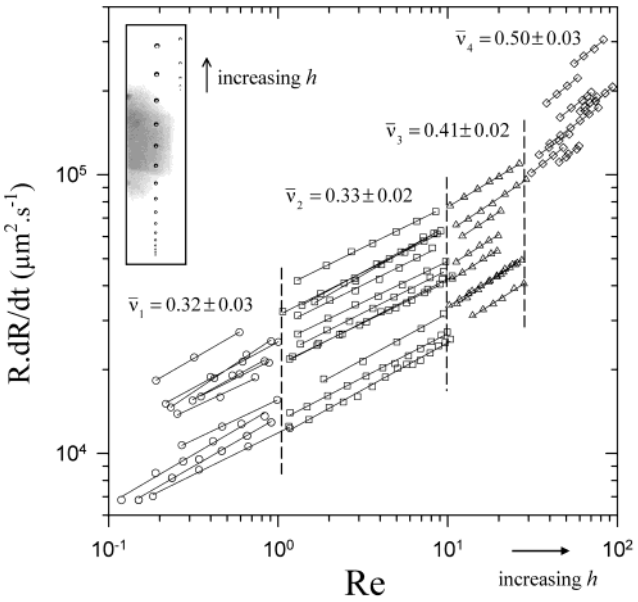

Figure 4. Experimental determination of the four average critical exponents of the fitted power laws, Sh(Re), experienced by bubbles of various bubble trains, into each of the four ranges of Re previously defined.

R and of the bubble growth rate, $\dot{R}$, during ascent enables the experimental determination of the Sherwood number all along the bubble rise, except for the numerical prefactor.

At low Re (Re < 1), mass transfer eqs 4 are analytically solvable for both rigid and fluid sphere boundary conditions. But, at higher Re (Re > 1), mass transfer equations are not analytically solvable anymore, which has mainly restricted the previous studies on mass transfer phenomena at intermediate and high Re to experimental and numerical investigations. During the past decades, numerous empirical relationships have been proposed in the literature to correlate the Sherwood number experienced by a bubble in free rise with its Peclet number (indirectly its Reynolds number, since Pe = ScRe and since Sc is a constant depending only on some fluid parameters).

Exactly as we did with the drag coefficients, we retrieved different theoretical and empirical relationships previously derived for Sh, available for both rigid and fluid sphere conditions and in the whole range of Re experienced by champagne bubbles during ascent. The different relationships Sh(Re) were found in the book by Clift et al.[25] They are listed with their range of validity in Table 2 and plotted in Figure 3.

In Figure 3, the whole range of Re experienced by expanding and accelerating champagne bubbles (i.e., Re $\approx 10^{-1}-10^{2}$) was divided into four independent regions: $10^{-1}-1$, $1-10$, $10-30$, and $30-10^{2}$. Into each of these four ranges, both $Sh_{RS}(Re)$ and $Sh_{FS}(Re)$ have been plotted and very accurately fitted by power laws (with a correlation coefficient r^2 of better than 0.99). Consequently, into each of the four ranges of Re considered, mass transfers associated with both rigid and fluid sphere conditions can be characterized by two different and well-defined critical exponents, ν_{RS} and ν_{FS}, respectively. In Figure 3, the eight critical exponents of the eight respective power laws appear close to their corresponding curves.

Experimentally, since the numerical prefactor in eq 8 can be considered as a constant during the short time of a bubble rise, the variations of the Sherwood number experienced by an expanding champagne bubble are only attributed to variations of the term $R\dot{R}$ easily accessible all along the bubble rise with our experimental setup. Therefore, for each of the numerous bubble trains investigated, the term $R\dot{R}$ was determined along the bubble rise with increasing Re. Experimental results are plotted in Figure 4. For each given bubble train, in each of the four ranges of Re previously defined, the term $R\dot{R}$ was independently correlated with Re and also fitted by power laws. An average value of the experimental critical exponents found for each bubble train was calculated in each of the four ranges of Re considered. The four experimental average values of this exponent also appear in Figure 4, in the corresponding range of Re.

From Re $\approx$ 0.1 to Re $\approx$ 30, the experimental critical exponent is rather close to that of the rigid sphere limit, thus suggesting a transfer of CO_2 molecules through the bubble interface governed by rigid sphere boundary conditions. In the last range of Re, from Re $\approx$ 30 to Re $\approx$ 100, the experimental critical exponent significantly deviates from that of a rigid sphere to exhibit a value, $\bar{\nu}_4$

≈ 0.50, intermediate between that of a rigid sphere ($\nu_{RS} \approx 0.40$) and that of a fluid sphere ($\nu_{FS} \approx 0.57$). This result, based on the mass transfer theory, suggests a progressive change in the bubble surface state which seems to recover its interfacial mobility, as also suggested by the drag coefficient data of Figure 2. Nevertheless, the progressive gain of interfacial mobility indirectly evidenced by use of mass transfer equations seems to occur later (from Re $\approx$ 30) than that indirectly evidenced by use of the drag coefficients (from Re $\approx$ 1). Such a gap in the change of interfacial mobility detected by these two independent methods could maybe be explained by having a closer look at the different time scales involved in our problem.

3.3. Characteristic Time Scales for Changes in the Drag Coefficient, in the Sherwood and in the Reynolds Numbers of Ascending Bubbles. While rising through the liquid, bubbles increase in size and continuously accelerate. Bubbles therefore continuously modify the velocity and concentration fields in their close vicinity. Actually, the empirical relationships C_{RS}, C_{FS}, Sh_{RS}, and Sh_{FS} listed in Table 1 and in Table 2 were calculated and estimated in steady-state conditions, that is, assuming that the velocity and concentration fields have reached steady states. For expanding and continuously accelerating bubbles, as are champagne bubbles, steady-state conditions may not necessarily be reached as will be discussed below.

Takagi and Matsumoto[29] numerically analyzed the motion of bubbles released in a quiescent liquid and showed that the characteristic time required for the drag coefficient of a rising bubble of radius R to come within 5% of the drag coefficient at steady state is around

$$\tau_{C_D} \approx \frac{\rho R^2}{5\eta} \tag{9}$$

As concerns the mass transfer phenomenon at large Pe, the book by Clift et al.[25] reports a relationship between Sh and Pe available for unsteady state and for fluid sphere boundary conditions:

$$\mathrm{Sh}_{FS}(\tau) = \mathrm{Pe}^{1/2}\left(0.117 + \left(\frac{2}{\sqrt{\pi\tau}\mathrm{Pe}^{1/2}}\right)^5\right)^{1/5} \tag{10}$$

where $\tau = Dt/R^2$ is a dimensionless time, regarded as the ratio of real time to the time for diffusion to become established. It is sometimes called the Fourier number. For long times, τ tends toward infinity and Sh reaches its steady-state value. Therefore, the time τ required for Sh to come within x% of the steady-state value is accessible by replacing $\tau_x = Dt_x/R^2$ in eq 10 and by solving $\mathrm{Sh}(\infty)/\mathrm{Sh}(\tau_{x\%}) = 1 - x$. A characteristic time, which is expressed as follows, was obtained for Sh to come within 5% of its steady-state value:

$$\tau_{\mathrm{Sh(FS)}} \approx \frac{2R}{U} \tag{11}$$

Since our results on the drag coefficients and Sherwood numbers are presented as a function of the continuously increasing Reynolds number of expanding champagne bubbles, τ_{C_D} and τ_{Sh} are necessarily to be compared with the characteristic time of Re increase during the bubble rise, that is,

$$\tau_{\mathrm{Re}}^{-1} = \frac{1}{\mathrm{Re}}\frac{\mathrm{dRe}}{\mathrm{d}t} = \frac{1}{RU}\frac{\mathrm{d}(RU)}{\mathrm{d}t}$$

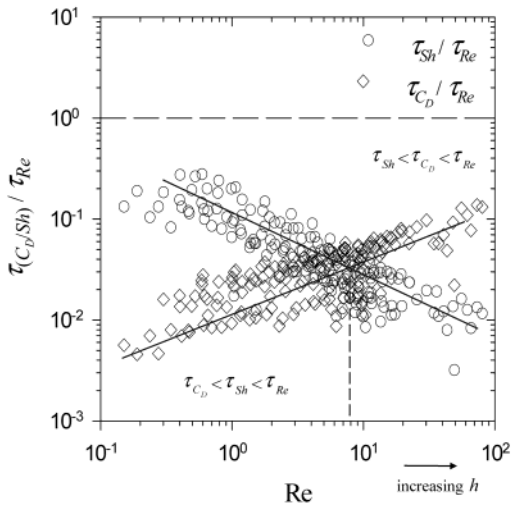

Figure 5. Ratios of the two characteristic time scales τ_{C_D} and τ_{Sh} to the characteristic time scale of Re increase τ_{Re}, plotted as a function of Re all along the bubble rise for numerous bubble trains.

In Figure 5, for numerous bubble trains, the ratios of τ_{C_D} and τ_{Sh} to τ_{Re} are plotted all along the bubble rise with increasing Re. Clearly, the time scales τ_{C_D} and τ_{Sh} are always below τ_{Re}, which means that although bubbles continuously expand and accelerate during ascent, the velocity and concentration fields around rising bubbles tend more quickly toward their steady-state value than Re increases. Moreover, below Re $\approx$ 10, $\tau_{C_D}/\tau_{Re} < \tau_{Sh}/\tau_{Re}$, whereas above Re $\approx$ 10, $\tau_{C_D}/\tau_{Re} > \tau_{Sh}/\tau_{Re}$. Therefore, we can assume that, in turn, the drag coefficient and the Sherwood number have reached their steady-state values, above and below Re $\approx$ 10, respectively. As a result, below Re $\approx$ 10, the normalized drag coefficient C_D*(Re) already detects a gain of interfacial mobility, although Sh(Re) does not "feel" it yet, as previously suggested by comparing Figures 2 and 4. Above Re $\approx$ 10, the situation reverses and Sh(Re) becomes a better candidate than C_D*(Re) to detect a change of interfacial mobility.

Therefore, the gap in the change of interfacial mobility detected by measuring, at the same time, the drag coefficient and the Sherwood number of ascending bubbles could be explained by comparing the relative duration of corresponding time scales, τ_{C_D} and τ_{Sh}, with τ_{Re}. The close examination of the time scales involved in our problem finally suggests that steady-state conditions are reached, in turn, respectively for hydrodynamic and mass transfer phenomena. Therefore, it confirms the probable transient regime in terms of interfacial mobility experienced by ascending champagne bubbles.

To complete this work on the surface state of ascending champagne bubbles, we were tempted to compare our experimental data on ascending champagne bubbles with some theoretical investigations on the surfactant flux toward a moving sphere, suited to the case of expanding bubbles rising in low dilute surfactant solutions.

3.4. The Champagne Bubble Surface State Ruled by a Probable Competition between Surfactant Adsorption and Bubble Growth. During ascent, sur-

(26) Magnaudet, J.; Rivero, B.; Fabre, J. *J. Fluid Mech.* **1995**, *284*, 97−135.
(27) Maxworthy, T.; Gnann, C.; Kürten, M.; Durst, F. *J. Fluid Mech.* **1996**, *321*, 421−441.
(28) Abdel-Alim, A. H.; Hamielec, A. E. *Ind. Eng. Chem. Fundam.* **1975**, *14*, 308−312.
(29) Takagi, S.; Matsumoto, Y. *Proceedings of the ASME Summer Meeting on Numerical Methods for Multiphase Flow*; Crow, I. G., et al., Eds.; 1996; pp 575−580.

face-active substances accumulate at the bubble interface and contribute to its rigidifying. However, at the same time, the champagne bubble continuously grows as a result of supersaturating. Therefore, the area of the bubble interface increases, thus offering still more surface to the adsorbed materials. Bubbles experience a competition between two opposing effects. The parameter which controls the bubble surface state is its surface concentration of contaminants, denoted $\Gamma = M/A$, which is the ratio of the mass M of contaminants adsorbed to the bubble area. The variation of the bubble surface concentration with time, on expanding bubbles, is governed by the following equation:

$$\frac{d\Gamma}{dt} = \frac{1}{A}\left(\frac{dM}{dt}\right)_A - \frac{M}{A^2}\left(\frac{dA}{dt}\right)_M \qquad (12)$$

On the right-hand side of eq 12, the first term is the rate at which surfactants adsorb on the rising bubble and the second term is the rate of dilatation of the bubble area. Therefore, the variation with time of the surface concentration of contaminants on ascending bubbles depends on the ratio of the two terms on the right-hand side of eq 12. Finally, the variation with time of the surface concentration of contaminants on ascending bubbles is ruled by the ratio of the characteristic time scale of bubble expansion to the characteristic time scale of surfactant adsorption, respectively

$$\tau_{exp}^{-1} = \frac{1}{A}\frac{dA}{dt} = \frac{2\dot{R}}{R} \quad \text{and} \quad \tau_{ads}^{-1} = \frac{1}{M}\frac{dM}{dt} \qquad (13)$$

To complete this set of experiments on expanding champagne bubble dynamics, time scales of bubble expansion and surfactant adsorption are to be compared.

The time scale of bubble expansion, τ_{exp}, is easily experimentally accessible by measuring R and $\dot{R}$ all along the bubble rise, for each given bubble train.

As concerns the adsorption kinetics of surfactants, we retrieved theoretical calculations of diffusive and convective transport of solutes toward a bubble in free rise. At low Re, since ascending champagne bubbles behave as rigid spheres, we retrieved a calculation conducted by Levich[2] for rigid sphere boundary conditions,

$$\frac{dM}{dh}\Big|_{RS} \approx AC(\mathrm{Pe})^{-2/3} \approx AC\left(\frac{D_S}{2RU}\right)^{2/3} \qquad (\mathrm{Re} < 1) \quad (14)$$

where M, h, A, C, D_S, R, and U are the mass of adsorbed surfactants along the bubble rise, the traveled distance, the bubble area, the bulk concentration of surfactants, the bulk diffusion coefficient of surfactants, and the bubble radius and its velocity of rise, respectively.

At higher Re, since ascending champagne bubbles progressively exhibit higher interfacial mobility, we retrieved a theoretical result derived by Yang et al.[30] for fluid sphere boundary conditions, which led to an evolution of the mass of surface-active compounds adsorbed with the traveled distance ruled by

$$\frac{dM}{dh}\Big|_{FS} \approx AC(\mathrm{Pe})^{-1/2} \approx AC\left(\frac{D_S}{2RU}\right)^{1/2} \qquad (\mathrm{Re} \gg 1) \quad (15)$$

The time scale for surfactant adsorption can be evaluated as follows:

$$\tau_{ads}^{-1} = \frac{1}{M}\frac{dM}{dt} = \frac{1}{M}\frac{dM}{dh}\frac{dh}{dt} = \frac{1}{M}\frac{dM}{dh}U \qquad (16)$$

As a result, by replacing dM/dh in eq 16 by its expression given in eqs 14 and 15, the ratios of the two characteristic time scales become, respectively at low Re for rigid sphere conditions and at high Re for fluid sphere conditions:

$$\begin{cases} \dfrac{\tau_{exp}}{\tau_{ads}}\Big|_{RS} \approx \dfrac{C}{\dot{R}\Gamma}(D_S)^{2/3}(UR)^{1/3} & (\mathrm{Re} < 1) \\ \dfrac{\tau_{exp}}{\tau_{ads}}\Big|_{FS} \approx \dfrac{C}{\dot{R}\Gamma}(D_S UR)^{1/2} & (\mathrm{Re} \gg 1) \end{cases} \qquad (17 \text{ and } 18)$$

Finally, let us test the compatibility of relations 17 and 18 with our experimental observations on the bubble surface state as reported in Figures 2 and 4.

Up to now, the pool of surface-active macromolecules in a typical champagne wine is far from perfectly known. It was nevertheless recently demonstrated that most of the surface-active macromolecules of champagne wines showed molecular masses in the range of 10^4-10^5 (mostly composed of proteins and glycoproteins[31,32]). We will retrieve in eqs 17 and 18 a diffusion coefficient characteristic of high molecular mass proteins in water, $D_S \approx 10^{-11}\ \mathrm{m^2\ s^{-1}}$. At low Re, since Figures 2 and 4 both suggest rigid sphere boundary conditions, we will retrieve in eq 17 the average surface concentration, $\Gamma_{RS} \approx 10^{-6}\ \mathrm{kg\ m^{-2}}$, corresponding to the order of magnitude of the equilibrium surface concentration of proteins at the air/water interface. At higher Re, since Figures 2 and 4 suggest a progressive gain of interfacial mobility of ascending champagne bubbles, we will retrieve in eq 18 an average surface concentration, $\Gamma \approx 10^{-7}\ \mathrm{kg\ m^{-2}}$, corresponding to a very low surface coverage of proteins. Finally, by inserting at low and high Re in eqs 17 and 18, respectively, experimental data for U, R, and $\dot{R}$ for each given bubble train, the measured bulk concentration of proteins, $C \approx 5 \times 10^{-3}\ \mathrm{kg\ m^{-3}}$, and the diffusion coefficient characteristic of proteins, D_S, the expected ratios of the two characteristic time scales, $(\tau_{exp}/\tau_{ads})_{RS}$ and $(\tau_{exp}/\tau_{ads})_{FS}$, can be approached. These ratios are presented in Figure 6 at low and high Re and for both rigid and fluid sphere boundary conditions.

At low Re, $(\tau_{exp}/\tau_{ads})_{RS}$ is much lower than unity. This means that the rate of dilatation of the champagne bubble area exceeds the rate at which surfactants adsorb on the rising bubble. Consequently, the bubble interface progressively and inexorably recovers its interfacial mobility as suggested in Figures 2 and 4 at low and intermediate Re. At higher Re, $(\tau_{exp}/\tau_{ads})_{FS}$ is significantly higher than unity. Therefore, the rate of dilatation of the champagne bubble area becoming lower than the rate at which surfactants adsorb on the rising bubble, the situation should reverse. Consequently, after a first experimentally detected transient regime where the rising bubble interface changes from that of a rigid to that of a fluid sphere, the interfacial mobility of ascending champagne bubbles should be seen to decrease, which is clearly not observed from the observation of both C_D*(Re) and Sh(Re) in Figures 2 and 4.

We propose two hypotheses to explain this difference. First, due to flow interactions between successive bubbles,

(30) Yang, S.-M.; Han, S. P.; Hong, J. J. *J. Colloid Interface Sci.* **1995**, *169*, 125−134.

(31) Perron, N.; Cagna, A.; Valade, M.; Bliard, C.; Aguié-Béghin, V.; Douillard, R. *Langmuir* **2001**, *17*, 791−797.

(32) Puff, N.; Marchal, R.; Aguié-Beghin, V.; Douillard, R. *Langmuir* **2001**, *17*, 2206−2212.

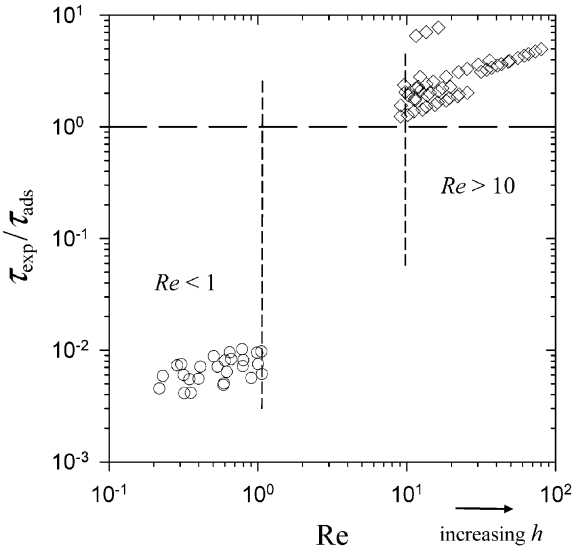

Figure 6. Ratio of the characteristic time scale of bubble expansion to the characteristic time scale of surfactant adsorption plotted as a function of Re all along the bubble rise for numerous bubble trains.

the surfactant adsorption dynamics on bubbles rising in-line could be rather different from that of a single bubble, thus making obsolete the use of eqs 14 and 15. Second, above Re ≈ 10, the characteristic times for C_D and Sh to come within 5% of their steady-state values could forbid the indirect detection of a possible loss of interfacial mobility. But, since $\tau_{Sh} \ll \tau_{Re}$ at high Re, as seen in Figure 5, this possible loss of interfacial mobility following the first "cleaning" regime could probably become accessible by measuring Sh(Re) at Re > 100 (with bubble trains longer than 10 cm). However, the onset of bubble oscillations, due to wake instabilities from Re ≈ 250, would certainly become very quickly a new problem to face.[33]

4. Conclusions

By combining a new set of experimental data on the drag coefficient and the Sherwood number of ascending champagne bubbles with a close examination of the different time scales involved in our system, we suggest that the interfacial mobility of ascending champagne bubbles experiences a transient regime, where the bubble behavior changes from that of a rigid to that of a fluid sphere. This transient regime strongly suggests that the rate at which surface-active molecules adsorb on and rigidify the rear part of an ascending bubble remains lower than the rate at which the bubble interface expands by diffusion of carbon dioxide molecules. Contrary to bubbles of fixed or shrinking radii, expanding champagne bubbles would progressively "clean up" themselves by a progressive dilution of the adsorbed surface-active compounds due to the continuous expansion of the bubble area.

Since the present work relies on reasoning with dimensionless numbers, we are tempted to extend the conclusions of this article to the more global case of bubbles rising in low dilute surfactant solutions, at intermediate Reynolds and high Peclet numbers, and expanding at growth rates of several hundreds of micrometers per second.

(33) Wu, M.; Gharib, M. *Phys. Fluids* **2002**, *14*, 49−52.

Acknowledgment. Thanks are due to the Europôl'Agro Institute, to the "Association Recherche Oenologie Champagne Université", and to Champagne Moët & Chandon, Pommery and Verrerie Cristallerie d'Arques, for supporting our research and to Michèle Vignes-Adler for valuable discussions.

Nomenclature

A = bubble area, m^2
c_0 = concentration of dissolved CO_2 molecules close to the bubble interface, molecules m^{-3}
c_∞ = concentration of dissolved CO_2 molecules in the champagne bulk far from the bubble surface, molecules m^{-3}
C = concentration of surface-active materials in the champagne bulk, kg m^{-3}
C_D = drag coefficient experienced by a bubble
C_D* = normalized drag coefficient experienced by a bubble as defined in eq 3
D = diffusion coefficient of dissolved CO_2 molecules in the liquid bulk, $\approx 1.5 \times 10^{-9}$ m^2 s^{-1}
D_S = diffusion coefficient of surface-active macromolecules (primarily composed of proteins and glycoproteins) in the liquid bulk, $\approx 10^{-11}$ m^2 s^{-1}
f = frequency of bubble detachment from nucleation sites, s^{-1}
g = acceleration due to gravity, 9.8 m s^{-2}
k_B = Boltzman constant, 1.38×10^{-23} J K^{-1}
K = mass transfer coefficient, m s^{-1}
m = added mass of a bubble, kg
M = mass of surface-active materials adsorbed at the surface of a rising bubble, kg
n = index affected to a bubble of a bubble train
N = number of CO_2 molecules
P_0 = atmospheric pressure, $\approx 10^5$ N m^{-2}
P_B = pressure inside a bubble, N m^{-2}
Pe = Peclet number, $2RU/D$=ScRe
R = bubble radius, m
$\dot{R}$ = bubble growth rate dR/dt, m s^{-1}
R_0 = bubble radius at detachment, m
Re = Reynolds number, $2\rho RU/\eta$
Sc = Schmidt number, $\eta/D\rho \approx 10^3$
Sh = Sherwood number, $2KR/D$
t = time, s
T = period of bubble formation, $1/f$, s
U = bubble velocity, m s^{-1}
V = bubble volume, m^3
η = champagne dynamic viscosity, 1.66×10^{-3} kg m^{-1} s^{-1}
ρ = fluid density, $\approx 10^3$ kg m^{-3}
θ = temperature, K
Γ = surface concentration of surface-active materials on a rising bubble, kg m^{-2}
Γ_{RS} = surface concentration of surface-active materials on a rising bubble showing rigid sphere boundary conditions, $\approx 10^{-6}$ kg m^{-2}
τ = Fourier number, regarded as the ratio of real time to the time for diffusion to become established, $\tau = Dt/R^2$
τ_{ads} = characteristic time of surfactant adsorption kinetics on ascending bubbles, s
τ_{exp} = characteristic time of bubble expansion during ascent, s
τ_{C_D} = characteristic time required for the drag coefficient of a rising bubble to come within 5% of the drag coefficient at steady state, s
τ_{Re} = characteristic time of Re increase, s
τ_{Sh} = characteristic time required for the Sherwood number of a rising bubble to come within 5% of the Sherwood number at steady state, s

Subscripts

RS = rigid sphere boundary conditions
FS = fluid sphere boundary conditions

LA026594W